

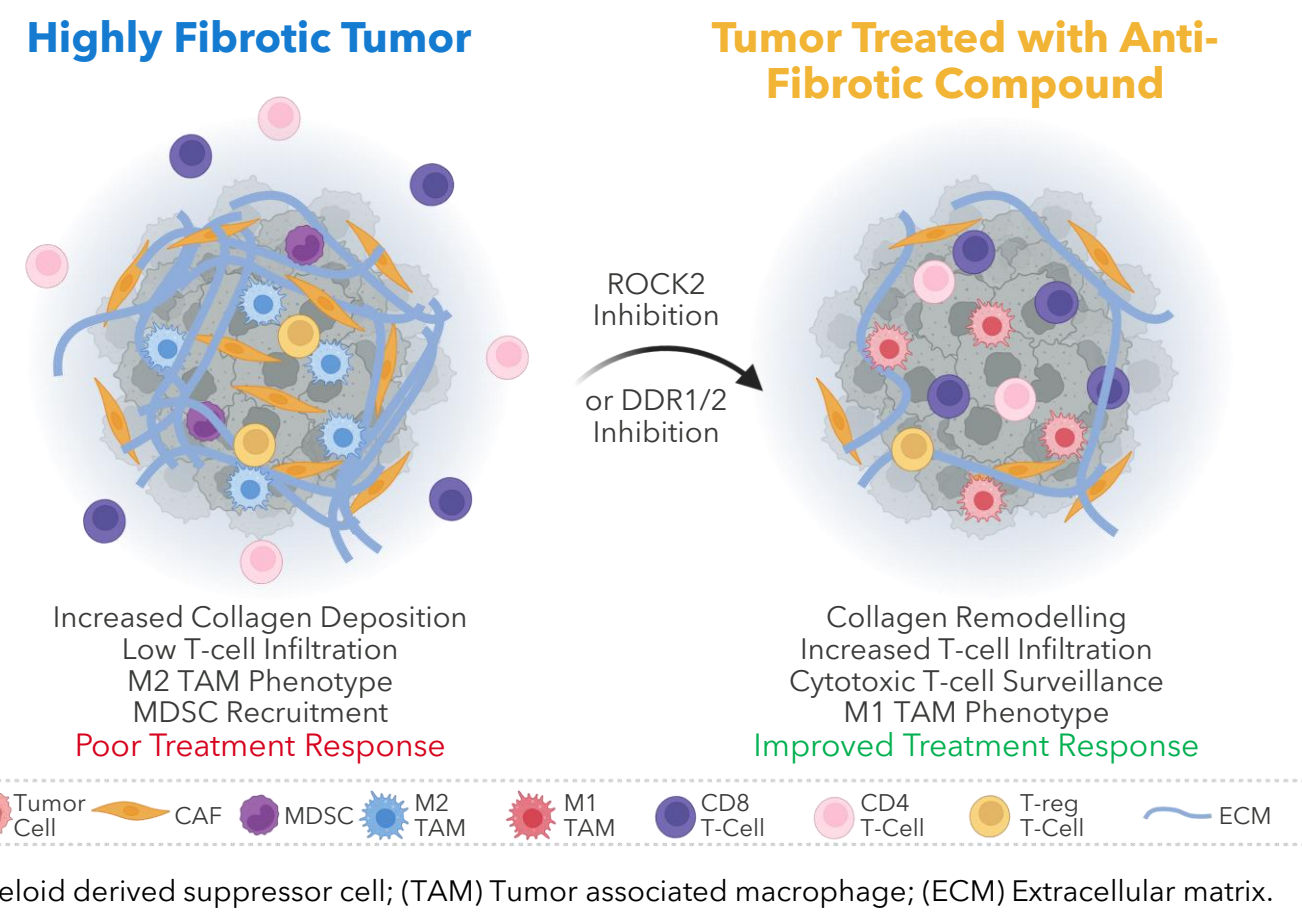
# Targeting Tumor Fibrosis with Small Molecule Inhibitors of ROCK2 or DDR1/2 Improves Therapy Response in Preclinical Models of PDAC & TNBC



Daniel J Wilcock<sup>1</sup>, Dorottya Keppel<sup>1</sup>, Benjamin McLean<sup>2</sup>, Sean Porazinski<sup>3</sup>, Eimear Flanagan<sup>1</sup>, Catherine Eagle<sup>1</sup>, Kay Eckersley<sup>1</sup>, Jack Lloyd-Weston<sup>1</sup>, Ana Varela Rodriguez<sup>1</sup>, Camille Gignoux<sup>1</sup>, James Ryan<sup>1</sup>, Michal Andra<sup>1</sup>, Nicolas E.S. Guisot<sup>1</sup>, Inder Bhamra<sup>1</sup>, Marina Pajic<sup>2,3</sup>, Clifford D Jones<sup>1</sup>, Caroline Philips<sup>1</sup>, Richard Armer<sup>1</sup>

## Introduction

- The critical role of the tumor-stromal microenvironment (TME) in driving tumor progression and modulating treatment response to chemo-, radio- and immunotherapy is well established.
- Tumor infiltrating stromal cells provide an additional layer of heterogeneity modulating extracellular matrix (ECM) deposition, exerting mechanical forces and secreting a milieu of factors leading to intertumoral fibrosis.
- Here, we discuss effects of two anti-fibrotic small molecule inhibitors of Discoidin-domain receptors 1&2 (DDR1/2) and Rho-associated coiled-coil containing protein kinase 2 (ROCK2) respectively, which have both demonstrated anti-fibrotic efficacy in preclinical mouse models of kidney and lung fibrosis (in-house data).
- ROCK2 expression has been shown to be increased in pancreatic cancer<sup>1</sup> and targeting of ROCK using Fasudil has been shown to potentiate response to standard of care (SoC) chemotherapy<sup>2</sup>.
- Discoidin domain receptors 1 and 2 (DDR1/2) are emerging targets in oncology, complete genetic knockout (KO) or knockdown (KD) of either DDR1 or DDR2 in mouse syngeneic models increases anti-tumor immune infiltrate in the TME<sup>3,4</sup>.
- Targeting of DDR1/2 using non-selective inhibitors in combination with chemotherapy in genetically engineered mouse models (GEMM) of Lung & Pancreatic cancer increased anti-tumor efficacy and survival<sup>5,6</sup>.
- The data presented investigates the rationale of targeting intertumoral fibrosis through small molecule inhibition that could lead to improved therapy response in combination with SoC chemotherapy or immunotherapy in tumor types characterized by high stromal infiltrate and dense ECM deposition which often prove to be therapy refractive.



## Results

### Development of Selective ROCK2 and DDR1/2 Inhibitors

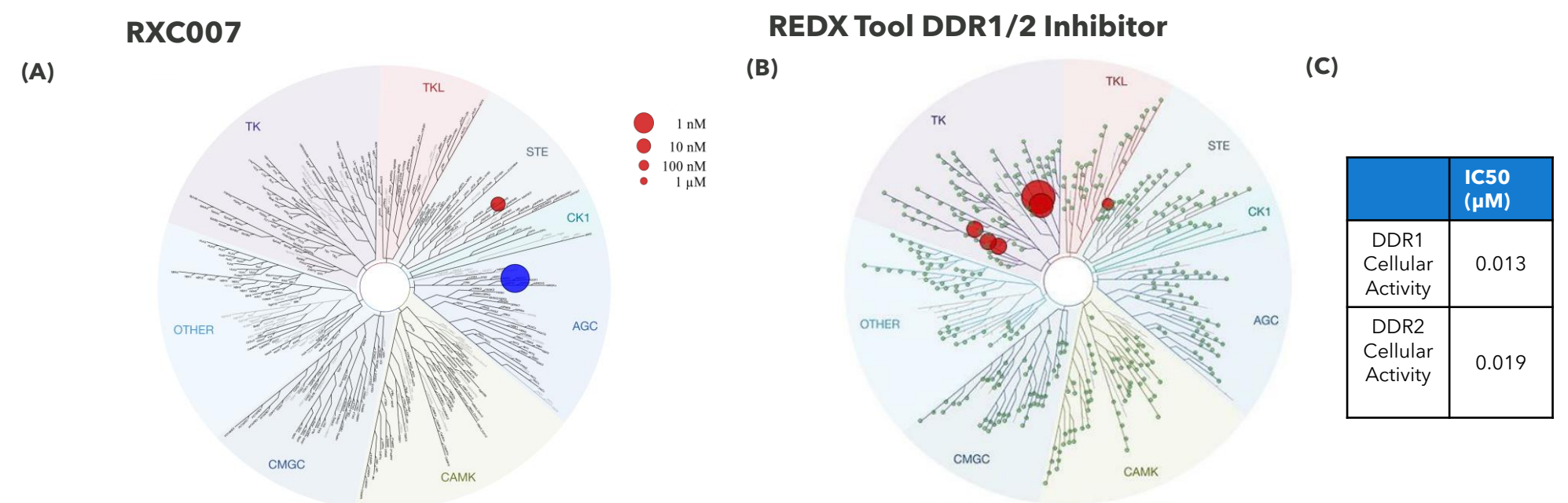


**Fig. 2: (A) TREEspot interaction map of RXC007 (B) TREEspot interaction map of REDX Tool DDR1/2 Inhibitor (C) Cellular activity IC50 values of REDX Tool DDR1/2 Inhibitor.** Kinase profiling carried out at Eurofins. (A) IC50 determination of RXC007 at Km ATP of the 20 kinases inhibited with >50% following 468-kinase panel at 10 µM. ROCK2 is the most potently inhibited kinase, >100-fold selectivity versus ROCK1 in biochemical assays. >100-fold selectivity against 468 kinases. (B) KINOMEScan profiling service showing percentage inhibition of 468 kinases assessing REDX tool DDR1/2 inhibitor at 1000nM. Only 8 kinases, including DDR1 and DDR2 were inhibited >90%. (C) The cellular IC50 of the REDX tool DDR1/2 inhibitor was assessed in HEK293 cells overexpressing full length DDR1 or DDR2. HEK293 cells overexpressing DDR1 or DDR2 were stimulated by collagen I to activate DDR1 or DDR2 prior to dosing with compound, phosphorylation of DDR1 or DDR2 was assessed by ELISA and IC50s calculated.

### ROCK2 inhibition reduces collagen content in a KPC PDAC model

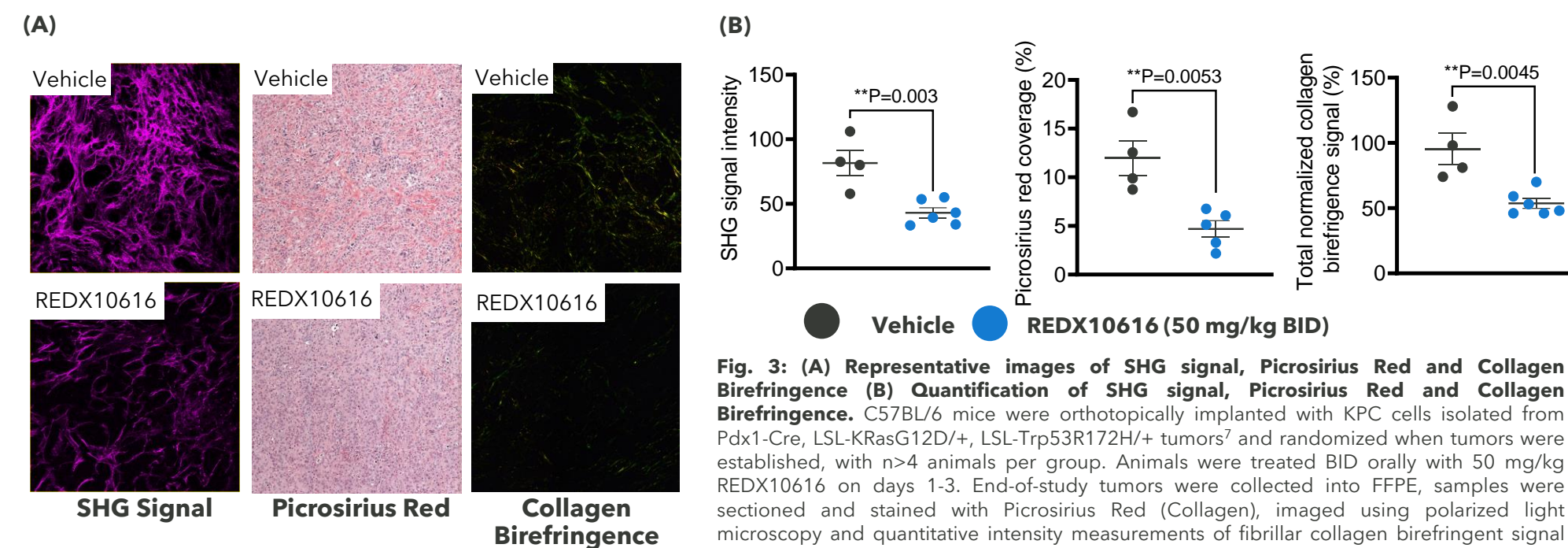


**Fig. 3: (A) Representative images of SHG signal, Picrosirius Red and Collagen Birefringence (B) Quantification of SHG signal, Picrosirius Red and Collagen Birefringence.** C57BL/6 mice were orthotopically implanted with KPC cells isolated from Pdx1-Cre, LSL-KRasG12D/+; LSL-Trp53R172H/+ tumors and randomized when tumors were established, with n>4 animals per group. Animals were treated BID orally with 50 mg/kg REDX10616 on days 1-3. End-of-study tumors were collected into FFPE, samples were sectioned and stained with Picrosirius Red (Collagen), imaged using polarized light microscopy and quantitative intensity measurements of fibrillar collagen birefringent signal were carried out on polarized light images using ImageJ. SHG signal was acquired using a 25x 0.95 NA water objective on an inverted Leica DMI 6000 SP8 confocal microscope and the intensity measured with Image J. Statistical analysis carried out using unpaired T-test in GraphPad Prism.

### ROCK2 inhibition alters the tumor immune microenvironment in a KPC PDAC model

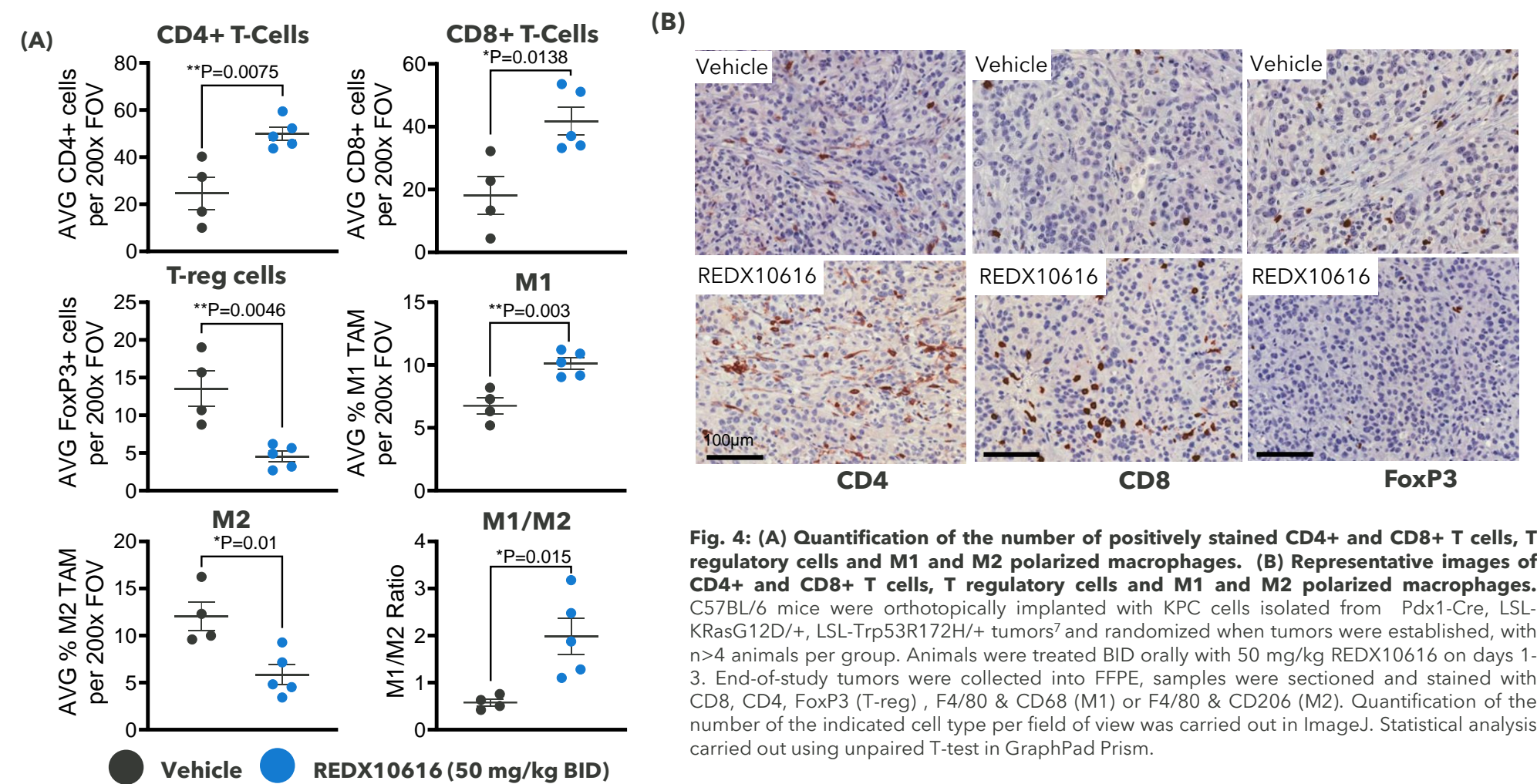


**Fig. 4: (A) Quantification of the number of positively stained CD4+ and CD8+ T cells, T regulatory cells and M1 and M2 polarized macrophages. (B) Representative images of CD4+ and CD8+ T cells, T regulatory cells and M1 and M2 polarized macrophages.** C57BL/6 mice were orthotopically implanted with KPC cells isolated from Pdx1-Cre, LSL-KRasG12D/+; LSL-Trp53R172H/+ tumors and randomized when tumors were established, with n>4 animals per group. Animals were treated BID orally with 50 mg/kg REDX10616 on days 1-3. End-of-study tumors were collected into FFPE, samples were sectioned and stained with CD8, CD4, FoxP3 (T-reg), F4/80 & CD68 (M1) or F4/80 & CD206 (M2). Quantification of the number of the indicated cell type per field of view was carried out in ImageJ. Statistical analysis carried out using unpaired T-test in GraphPad Prism.

### RXC007 increases survival in combination with Gemcitabine/Abraxane in metastatic and High-ECM patient-derived PDAC

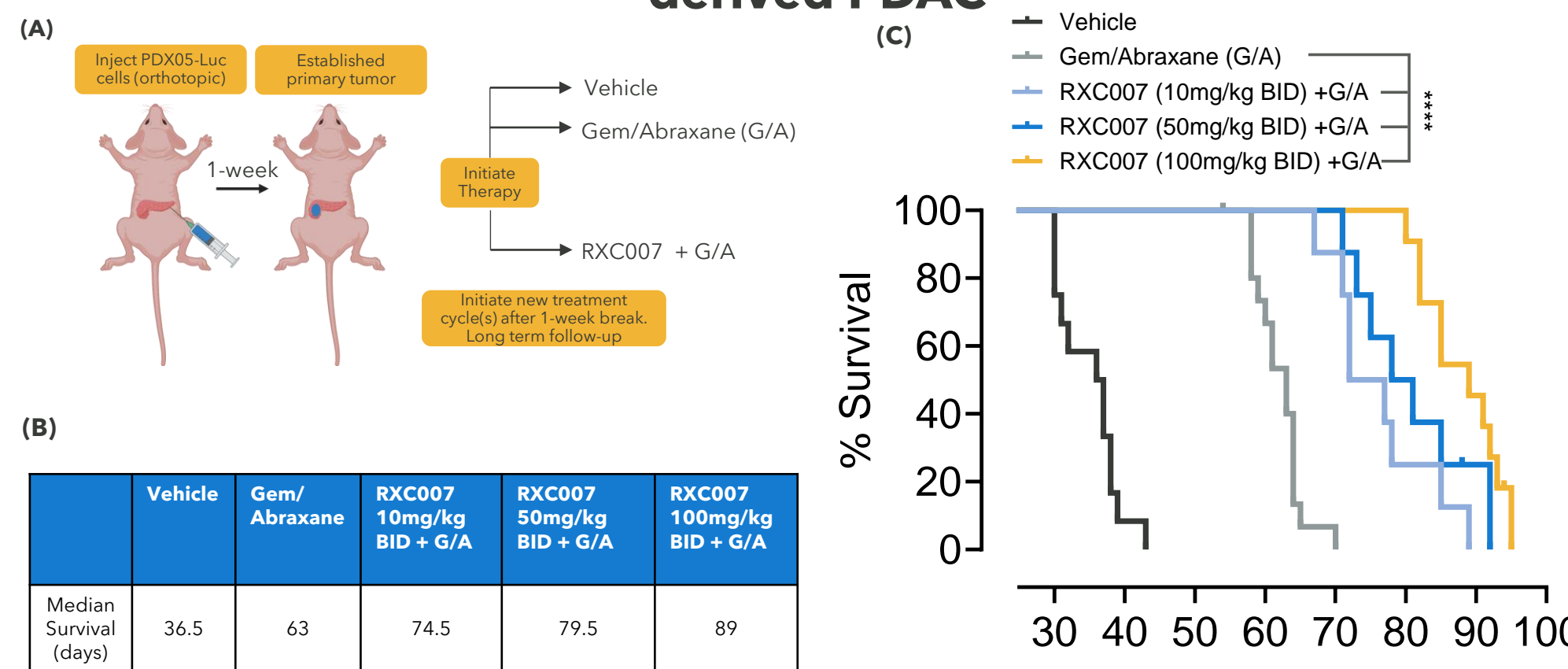


**Fig. 5: (A) Schematic of the orthotopic implantation and treatment groups in the PDX05-Luc mouse model (B) Table of the median survival of each treatment group (C) Kaplan Myer survival plot.** NOD/SCID IL2 gamma null (NSG) mice were orthotopically implanted with the PDX05-Luc patient derived cell line and randomized when tumors were established. Animals were treated BID orally with indicated dose of RXC007 and QW by intraperitoneal injection with 30mg/kg Abraxane and 70 mg/kg Gemcitabine. Vehicle n=12; Gem/Abraxane (G/A) n=5; RXC007 (10mg/kg BID) + G/A n=8; RXC007 (50mg/kg BID) + G/A n=7; RXC007 (100mg/kg BID) + G/A n=8. (B,C) Statistical analysis of survival carried out using Mantel-Cox test in GraphPad Prism \*\*\*\*p<0.0001.

### ROCK2 inhibition increases survival in FOLFIRINOX resistant patient-derived PDAC model

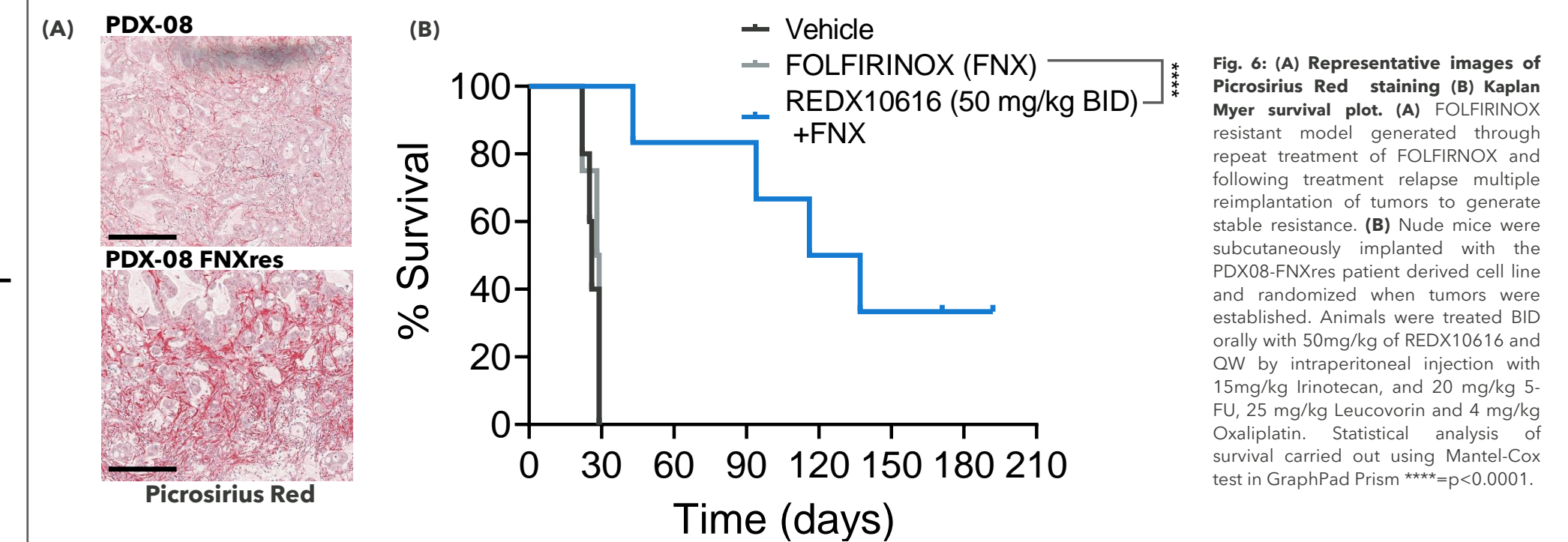


**Fig. 6: (A) Representative images of Picrosirius Red staining (B) Kaplan Myer survival plot.** (A) FOLFIRINOX resistant model generated through repeat treatment of FOLFIRINOX and following treatment relapse multiple reimplantation of tumors to generate stable resistance. (B) Nude mice were subcutaneously implanted with the PDX08-FNXres patient derived cell line and randomized when tumors were established. Animals were treated BID orally with 50mg/kg of REDX10616 and QW by intraperitoneal injection with 15mg/kg Irinotecan, and 20 mg/kg 5-FU, 25 mg/kg Leucovorin and 4 mg/kg Oxaliplatin. Statistical analysis of survival carried out using Mantel-Cox test in GraphPad Prism \*\*\*\*p<0.0001.

### DDR1/2 inhibition increases survival and alters the tumor immune microenvironment in combination with anti-PD1 in TNBC model

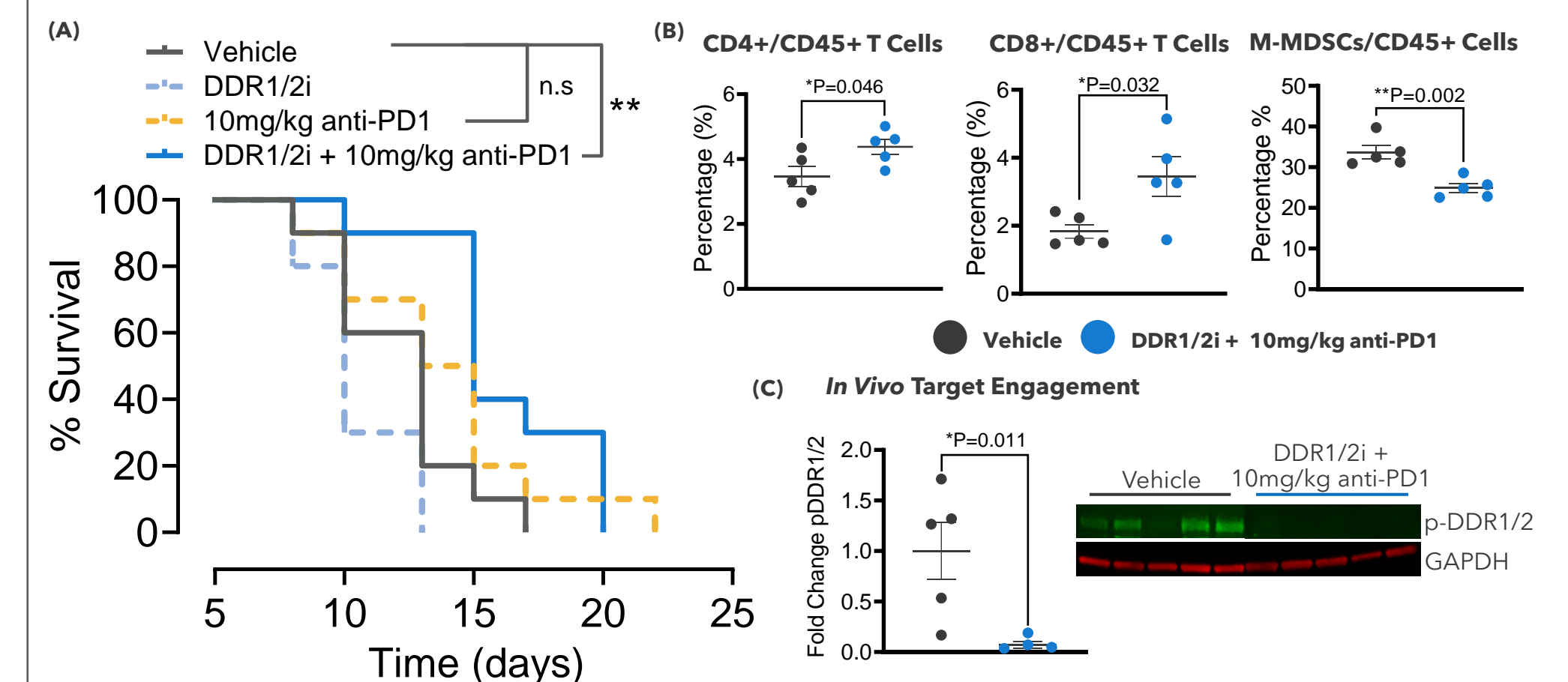


**Fig. 7: (A) Kaplan Myer survival plot (B) Quantification of indicated immune cell infiltration into the tumor as determined using flow cytometry (C) Western blot image and quantification of p-DDR1/2 levels.** In vivo studies were run at Syngene Discovery. C57BL/6 mice were orthotopically implanted with the TNBC E0771 cell line and randomized when tumors reached an average volume of 100mm<sup>3</sup> with 10 animals per group (A) or 5 animals per group (B,C). Animals were treated BID orally with a DDR1/2 inhibitor and 10 mg/kg BINV by interperitoneal injection of anti-PD1. (A) Statistical analysis of survival carried out using Mantel-Cox test in GraphPad Prism \*\*p=0.0045. (B) After 7-days of drug treatment fresh tumors were collected, dissociated stained for flow cytometric analysis, gating for the indicated immune cell populations was as follows: CD4+ T-cells (CD45+, CD4+); CD8+ T-cells (CD45+, CD8+); M-MDSCs (CD45+, CD11b+, Ly6C+, Ly6G+). Statistical analysis carried out using unpaired T-test in GraphPad Prism. (C) After 7-days of drug treatment fresh tumors were collected and lysed for protein analysis, western blotting was carried out to assess the levels of phosphorylated DDR1/2, quantification was carried out in Image Studio (Licor) and statistical analysis carried out using unpaired T-test in GraphPad Prism.

## Conclusions

Highly selective small molecule inhibitors of Discoidin-domain receptors 1&2 (DDR1/2) and Rho-associated coiled-coil containing protein kinase 2 (ROCK2) have been developed in-house at Redx.

The ROCK2 inhibitor REDX10616, a close analogue of RXC007, altered both the stromal and immune compartments in the KPC PDAC model. REDX10616 monotherapy led to significant decreases in tumor fibrillar collagen content, as measured by Second harmonic generation (SHG) imaging and polarized light microscopy. Moreover, increased CD4+ & CD8+ T cell infiltrate, a reduction in T Regs and alteration of macrophage polarization was observed upon REDX10616 mono-therapy.

In a high-ECM and highly metastatic patient derived orthotopic model of PDAC the combination of ROCK2 inhibition with RXC007 and SoC chemotherapy (G/A) led to a dose dependent increase in survival when compared to chemotherapy alone.

In a chemo-resistant patient derived model, in which an increase in tumor collagen content is observed upon development of resistance, the addition of REDX10616 in combination with FOLFIRINOX re-sensitized the tumor to treatment and led to a striking increase in survival.

Using a tool DDR1/2 inhibitor in combination with anti-PD1 in the TNBC E0771 model led to an increase in survival when compared to the control group, an effect not observed upon single agent treatment. The combination also led to an increase in CD4+ and CD8+ T cells and a decrease in M-MDSCs in the tumors, compared to control animals.

The data presented here provides a rationale for clinical investigation of this approach to treatment.

## References

1. Rath et al. (2017) EMBO Molecular Medicine, 9(2); 2. Vennin et al. (2017) Science Translational Medicine, 9(384); 3. Tu et al. (2019) Science Advances, 5(2); 4. Zhong et al. (2019) Oncology Reports, 42(6); 5. Nokin et al. (2020), JCI Insight, 5(1); 6. Aguilera et al. (2017) Molecular Cancer Therapeutics, 16(11); 7. Hingorani et al. (2005) Cancer Cell, 7(5).